doi.org/10.36721/PJPS.2025.38.6.REG.12639.1

Construction and *in vitro*/ *in vivo* evaluations of pulse sustained release of verapamil hydrochloride delivery system

Wei Mi[1#], Tao Xiao[2#], Yang Xu[3], Jiapeng Wang[3], Yingshu Feng[4], Caleb Kesse Firempong[3], Yan Jiang[5], Haibing He[6,7]* and Hongfei Liu[2,3,7]*

[1]Jiangxi alpha hi-tech Pharmaceutical Co., Ltd, Pingxiang, P.R. China
[2]College of Pharmacy, Jiangxi University of Chinese Medicine, Nanchang, P.R. China
[3]College of Pharmacy, Jiangsu University, Zhenjiang, P.R. China;
[4]Zhenjiang Key Laboratory of Functional Chemistry, Institute of Medicine & Chemical Engineering, Zhenjiang College, Zhenjiang, P.R. China
[5]Sichuan Institute for Drug Control (Sichuan Testing Center for Medical Devices), Chengdu, P.R. China
[6]Department of Pharmaceutics, Shenyang Pharmaceutical University, Shenyang, P. R. China
[7]Jiangsu Haizhihong Biomedical Co., Ltd, Nantong, P.R. China

Abstract: To prepare a porous cation exchange resin excipient and a verapamil hydrochloride (VH) pulse sustained release suspension, and to evaluate its *in vitro* release and *in vivo* pharmacokinetics. Porous cation exchange resin was prepared using suspension polymerization and sulfonation reaction. A drug-resin complex was formed via impregnation and coating, then formulated into a suspension. *In vitro* release profiles and pharmacokinetics in Sprague-Dawley rats were investigated. The custom-made resin complied with the relevant requirements of the United States Pharmacopeia, with a 2.6-fold higher surface area and 1.5-fold greater exchange capacity than IRP69. Compared with a conventional VH tablet (T_{max} 2 h, $t_{1/2}$ 1.407 h), the suspension delayed T_{max} to 5 h and extended $t_{1/2}$ to 4.191 h, exhibiting both enteric dissolution and sustained release characteristics. The findings showed that a verapamil hydrochloride pulsatile release suspension prepared with custom-made porous cation exchange resin achieved controlled and sustained release, potentially improving adherence in cardiovascular therapy by better aligning with disease progression. It is also likely to reduce dosing frequency and plasma concentration fluctuations, offering significant clinical value in the personalized management of conditions such as hypertension and angina.

Keywords: Porous cation exchange resin; Polymerization; Pulse sustained release suspension; Verapamil hydrochloride

Submitted on 07-03-2024 – Revised on 11-12-2024 – Accepted on 20-05-2025

INTRODUCTION

Ion-exchange resin (IER) is an insoluble reticulated polymer compound with active ion-exchange groups. It features a three-dimensional framework, where functional groups are bound via covalent bonds and exchangeable ions are attached through ionic bonds. The resin can form a drug-resin complex through ion exchange by interacting with drugs of the same charge. Upon entering the human body, the drug-resin complex undergoes a reverse process to drug loading, in which the complex interacts with ions in bodily fluids, replacing and releasing the drug (Panraksa *et al*., 2019). The mechanism relies on the formation of ionic interactions between the drug molecules and the functional groups on the resin, which gradually break down under specific pH conditions, particularly in acidic environment. This process, known as ion-exchange release, enables a controlled release of the drug as ionic bonds are disrupted, allowing the drug to be released at a steady rate (Zhang *et al.*, 2022). Previous studies have indicated that the structural and ionic characteristics of IERs can be tailored to prolong drug release, improve therapeutic outcomes a nd reduce dosing frequency (Yuan *et al.*, 2023). Consequently, IERs provide an effective pathway for sustained-release formulations, and matching the dynamic pH conditions of the gastrointestinal tract and enhancing patient compliance (Li *et al*., 2021).

IERs are commonly used in oral and non-injectable formulations to prolong drug action, stabilize drug release and improve bioavailability (Rajesh and Popat, 2017; Qin *et al.*, 2016). In recent years, they have been extensively studied in the development of new drug delivery systems (DDS) and other biomedical applications, with an increasing number of DDS containing IERs being introduced into the market (Sivaneswari *et al.*, 2015). Based on the surface structure of microspheres, IERs can be classified into gel and porous types (Gaur *et al.*, 2014). The gel-type resin has low cross-linking, and no pore-forming agent is added during its preparation, whereas the porous-type resin has high cross-linking. A porous structure is formed by the addition of a pore-forming agent during the synthesis of microspheres. Porous IERs offer better exchange capacity and faster exchange rates compared to gel-type resins, making them more

**Corresponding author:* e-mail: 24575816@qq.com; articlepharmacyliu@163.com
#These authors contributed equally to this work and should be considered co-first authors.

promising for applications in the pharmaceutical field. Consequently, research into the preparation of porous resins is fast increasing (Zhou *et al.*, 2017).

Hypertension is a common cardiovascular and cerebrovascular disease with high mortality and disability rates (Yin *et al*., 2022). The number of hypertensive patients has significantly increased, making it increasingly important to adopt effective measures for the prevention and treatment of this condition (Aronow, 2020). Studies have shown that the onset of hypertension follows a clear circadian rhythm, and the key to managing this condition lies in timing the treatment in conjunction with circadian rhythm-based medication, which can greatly reduce its incidence (Leonova, 2020). Verapamil hydrochloride (VH), a voltage-dependent calcium channel blocker, is used to treat essential hypertension, angina pectoris, and ventricular arrhythmia. The drug has few contraindications and is suitable for all degrees of hypertension.

However, due to its short biological half-life and limited efficacy in treating hypertension, its clinical application is restricted (Faisal *et al*., 2024).To address these issues, various sustained-release (SR) formulations have been developed to provide more consistent plasma concentrations and reduce dosing frequency (Ramu *et al*., 2016). Studies have shown that SR verapamil preparations, such as matrix tablets and osmotic delivery systems, effectively prolong drug release, improve efficacy, and reduce side effects (Shaik *et al*., 2015; Mohammed and Babu, 2015). Additionally, an ionic gelation method has been used to develop verapamil hydrochloride nanoparticles formulated with chitosan and sodium alginate, aiming to enhance bioavailability and extend drug release (Moeed *et al*., 2021). IERs are particularly promising, as they can form ionic complexes with verapamil, and facilitating gradual drug release in the gastrointestinal tract through ion exchange processes. For instance, it has been demonstrated that verapamil-loaded IERs provide a stable release profile, reducing plasma concentration fluctuations and lowering the incidence of adverse effects associated with peak concentrations (Allaboun *et al.*, 2023). At present, most research on sustained-release formulations of verapamil hydrochloride primarily focuses on adjusting preparation methods and materials to achieve more favorable drug release profiles or bioavailability. However, there is limited research on formulations developed specifically based on the treatment characteristics of hypertension.

In this study, medical-grade porous cation exchange resin polystyrene sodium sulfonate was prepared using suspension polymerization (Rajesh *et al.*, 2015), sulfonation reaction (Lei *et al*., 2014), and other processes. Additionally, the self-made porous cation exchange resin was used as the sustained-release carrier, with verapamil hydrochloride serving as the model drug. The pulse-sustained-release suspension of verapamil hydrochloride was then prepared using impregnation and coating methods. The *in vitro* release behavior of the resin microcapsules and suspension, as well as pharmacokinetics in SD rats, were investigated. Our research aims to refine drug release kinetics by adjusting the resin properties and formulation parameters, thereby enhancing therapeutic stability and patient adherence compared to existing SR formulations.

MATERIALS AND METHODS

Materials

Verapamil hydrochloride was obtained from Wuhan Dongkangyuan Technology Co., Ltd. (China). Divinyl benzene was obtained from Sigma-Aldrich (America). N-heptane and Cyclohexanol were purchased from Shanghai Aladdin Bio-Chem Technology Co., Ltd. (China). Dichloromethane and ethanol were purchased from Xilong Scientific Co., Ltd. (China). Styrene, Benzoyl peroxide, Polyvinyl alcohol and other reagents were purchased from Sinopharm Chemical Reagent Co., Ltd. (China).

Animals

Twelve specific-pathogen-free (SPF) Sprague-Dawley (SD) rats (200 ± 20 g) of equal sexes were selected and purchased from the Experimental Animal Center of Jiangsu University. All experimental animals were housed at room temperature (25-30^{o}C) under a 12-hour light/dark cycle, with adequate ventilation and access to food and water ad libitum. The animal studies were performed strictly according to the standard protocol approved by Jiangsu University Animal Center.

Preparation of porous cation exchange resin

Synthesis of porous polystyrene microspheres

Polyvinyl alcohol (PVA) (2.0 g) was placed in a three-neck flask, and deionized water was added. The mixture was heated and stirred until the PVA dissolved, and then the sample was lowered to room temperature. A mixture of styrene (ST), divinylbenzene (DVB), benzoyl peroxide (BPO), and the pore-forming agent's toluene, n-heptane and cyclohexanol were added to the flask after thorough mixing. The temperature was raised to 70^{o}C for 3 hours, then to 80^{o}C for 5 hours, and finally to 95^{o}C for 2 hours. Afterwards, the porous polystyrene microspheres (PS-DVB porous microspheres) were obtained by filtration and separation. The samples were washed several times with pure water and methanol. Then the sample was extracted with acetone as the solvent in a Soxhlet apparatus for 24 hours and dried under vacuum.

Sulfonation and alkali exchange of porous microspheres

The PS-DVB porous microspheres were placed in a three-neck flask, and chloroform was added to swell the microspheres for 0.5 hour. Concentrated sulfuric acid was slowly added to the sample while stirring the mixture. The

mixture was thoroughly stirred, and the sulfonation reaction was carried out by heating to 60ºC for 3 hours. After the reaction, the product was transferred to a beaker filled with purified water, washed until neutral pH condition, and then filtered by suction. The sample was washed with acetone several times and dried to obtain PS-DVB porous sulfonated microspheres (SPS-DVB porous microspheres). Ten grams of SPS-DVB porous microspheres were weighed into a beaker, and 2-3 drops of phenolphthalein indicator were added. The sample was then titrated with a 10% NaOH solution as the titrant. When the phenolphthalein turned red without fading within 60 minutes, the mixture was stirred at room temperature for 1 hour. The sample was washed with plenty of pure water until becoming neutral and then dried. Finally, porous crosslinked polystyrene sodium sulfonate cation exchange resin (SPS-DVB-Na porous resin) was obtained.

Characterization of porous ion exchange resins

Fourier transform infrared spectroscopy (FTIR) was used to characterize the structure of the IER. The morphology and pore structure of the IER were observed using a Sigma 300 scanning electron microscope (SEM). The particle size distribution of the resin was measured with an MS 3000 laser particle size analyzer. The specific surface area and pore size distribution were determined using nitrogen adsorption-desorption and mercury intrusion methods. Sodium content and potassium exchange capacity were measured with a ContrAA300 atomic absorption spectrometer.

Preparation of drug resin complex

As a common method for drug-resin binding, the static drug loading method offers several advantages over the dynamic loading method (Liu *et al.*, 2021). Therefore, the static drug loading method was used in this study. VH (500 mg) was dissolved in 100 mL of purified water to obtain a drug solution with a concentration of 5 mg/mL. The solution was stirred evenly at 37ºC and an equal amount of the self-made cation exchange resin was added and thoroughly stirred. Samples were periodically collected, and the absorbance was measured at 278 nm using a UV spectrophotometer. The ion exchange reaction reached equilibrium when the drug concentration remained stable. The drug formulation was filtered, and the unbound drug adsorbed on the resin surface was washed away with purified water. The verapamil hydrochloride-resin complex (VRC) was obtained by drying. The formulae of drug exchange volume (Q) and drug utilization ratio (E) of ion exchange resin at different time points are as follows:

$$Q_t = \frac{(C_0 - C_t)\ V}{W_F} \quad (1)$$

$$E = \frac{(C_0 - C_t)}{C_0} \quad (2)$$

$$F = \frac{Q}{Q_\infty} \quad (3)$$

Where C_0 represents the initial concentration of VH (mg/mL), C_t is the concentration of VH at time t (mg/mL), W_F denotes the mass of ion exchange resin (mg), V refers to the volume of purified water (mL), Q_t is the drug load at time t (mg/mL), and Q_∞ represents the drug load at equilibrium (mg/mL).

Impregnation and coating of drug resin complexes

Impregnation of drug fiber complexes

When the drug-carrier resin is coated directly, the coated microcapsules may swell in the medium or human body, leading to rupture of the coating film and a sudden release, which can affect drug efficacy and potentially cause adverse reactions (Deng *et al*., 2020). To address this, PEG 4000 was used to impregnate the drug-carrier resin before coating (Han *et al*., 2023). The procedure was as follows: 2.5 g of PEG 4000 was added to 7.5 mL of deionized water to prepare a 25% (W/V) aqueous solution. The solution was heated in a 35ºC water bath until the PEG 4000 fully dissolved, after which the VRC was added and stirred for 0.5 hours. The sample was then dried, sieved, and the VRC was successfully impregnated.

Preparation of coated microcapsules

The impregnated VRC was coated using the emulsification and solvent evaporation method (Qu *et al*., 2019). The inner oil phase consisted of 30 mL of a methanol-acetone mixture (1:5), while the outer oil phase contained 80 mL of liquid paraffin. Span 80 was used as an emulsifier, and PEG 400 served as a dispersant. The mixture was stirred at 50ºC until the methanol and acetone were fully evaporated. The product was then washed with petroleum ether and dried. This process yielded verapamil hydrochloride resin-coated microcapsules (VRC-CM).

Preparation of pulse sustained release suspension

Glycerol (1 g), Xanthan gum (0.02 g), propylparaben (0.012 g), Avicel CL611 (0.6 g), orange essence (0.1 g) propylene glycol (1 g) and FD & C Yellow No. 6 (0.002 g) were added to VRC-CM (equivalent to 240 mg of VH) under continuous stirring to obtain 20 mL of verapamil hydrochloride pulse sustained release suspension.

Drug release

Detection wavelength

An appropriate amount of verapamil hydrochloride and resin were weighed and placed into separate volumetric flasks, then diluted to volume with purified water. After filtration through a 0.45 μm membrane, full-wavelength scanning was conducted within the range of 200-400 nm.

In vitro release conditions

To determine the optimal ionic environment, the release of the drug-resin complex was evaluated in NaCl, KCl, HCl, and deionized water media. Additionally, the effects of different NaCl concentrations (0.15 mol/L, 0.5 mol/L, and 1.0 mol/L) on drug release were evaluated.

Drug release profile of VRC

The release of VRC was determined *in vitro* using the paddle method as outlined in the fourth section of the Chinese Pharmacopoeia (2020 Edition). The release conditions were as follows: A temperature of 37ºC ± 0.5ºC, 900 mL of 0.15 mol/L NaCl solution as the medium, and a rotation speed of 100 rpm. Samples were collected at a predetermined time point, with 5 mL taken at each time, and the medium was replenished promptly after each sampling. The absorbance of the sample was measured at 278 nm after the sample was filtered through a 0.45 μm membrane, and the amount of release was calculated accordingly. Based on an investigation of various influencing factors, the optimal release conditions for the drug-loaded resin were determined. The evaluation method used was the f_2 similarity factor method (Xie *et al*., 2015):

$$f_2 = 50 \times \log\left\{\left[1 + (1/n)\sum_{t=1}^{n}(R_t - T_t)^2\right]^{-0.5} \times 100\right\} \quad (4)$$

Where n represents the number of samples, R_t and T_t refer to the cumulative drug release of VRC at time t under different release conditions, and f_2 is the similarity factor. An f_2 value of ≥ 50 indicates similar drug release behavior under both conditions, whereas an f_2 value of ＜50 indicates different release behaviors between the two conditions.

In vivo pharmacokinetic studies

Dosage regimen

The 12 SD rats were randomly and equally divided into experimental group and control group, with 6 rats per group. Twelve hours before drug administration, the rats were fasted and then administered the drug via a single intragastric dose of 50 mg/kg. The control group received ground commercial verapamil hydrochloride tablet (SINE), while the experimental group was given a self-made verapamil hydrochloride pulse-sustained release suspension. After administration, 0.3 mL of blood was collected from the anterior venous plexus at different times (1, 2, 3, 4, 5, 6, 7, 8, 9, 10, 12, and 24 hours). The blood samples were placed in centrifuge tubes containing sodium heparin and allowed to stand for 30 minutes. Following centrifugation at 3700 rpm, the plasma supernatant was removed and stored at -20ºC for future analysis.

Preparation of plasma samples

An internal standard solution of diltiazem hydrochloride (120 μg/mL) and phosphate buffer solution (100 μL, pH 5.0) were added to 200 μL of the plasma sample and mixed for 30 seconds using a vortex mixer. Subsequently, 4 mL of the extraction solution (n-hexane-isopropanol, 98:2) was added, followed by vortex mixing for an additional 3 minutes. The sample was then centrifuged at 3700 rpm for 10 minutes, and 3 mL of the supernatant was collected. To the supernatant, 200 μL of 0.01 mol/L HCl solution was added and vortexed for 3 minutes, followed by centrifugation at 3700 rpm for 10 minutes. The filtrate was obtained through a 0.45 μm organic filter membrane and then injected into HPLC for drug content determination.

The chromatographic conditions for plasma sample testing were as follows: chromatographic column, Diamonsil-C_{18} (4.6 mm×250 mm, 5 μm, 100 A); mobile phase, acetonitrile-water (40:60, with 0.35% triethylamine in the water phase and phosphoric acid to adjust the pH to 4.0); detection wavelength, 278 nm; flow rate, 1.0 mL/min; injection volume, 20 μL; and column temperature, 40ºC.

Pharmacokinetic data analysis

DAS2.0 software was used to model the relationship between plasma concentration and time, and the optimal compartment model was also determined. Based on the fitting results, BAPP software was used to analyze the changes in blood drug concentration over time of each SD rat in the experimental and control groups. The pharmacokinetic parameters for each SD rat were calculated, and the average values were obtained.

Pharmacokinetic data analysis

Data were obtained in triplicates (at least) and expressed as mean ± standard deviation (SD). Statistical differences between mean values were determined and compared using one-way ANOVA with the help of SPSS v-20.0 (IBM, Armonk, NY, USA). Results with $p<0.05$ were considered statistically significant.

RESULTS

Self-made resin characterization

FTIR

The infrared spectrum of self-made cation exchange resin was consistent with that of the imported IRP69 resin, and the cation exchange resin polystyrene sodium sulfonate was successfully synthesized (Fig. 1).

SEM images

The results of the SEM analysis showed that the resin had a good spherical shape, and a uniform pore structure was visible on the resin surface at high magnification (Fig. 2).

Pore diameter and specific surface area

According to the adsorption and desorption curves and pore size distribution, the average pore size and specific surface area of the resin were 3.545 nm and 2.984 m^2/g, respectively, as calculated using the BJH and BET methods (Fig. 3).

Thermogravimetric characterization

PS-DVB gel microspheres underwent two decomposition processes (Fig. 4a). There was no significant weight loss around 100ºC, which indicated that the sample contained minimal water. The first stage of decomposition occurred between 190ºC and 270ºC, with a mass change of 29.8%,

which was attributed to the breakdown of small molecular monomers, such as porogens. The second decomposition stage occurred from 330ºC to 450ºC, with a mass change of 70.11%. This weight loss was caused by the decomposition and cleavage of the polymer's main chain, styrene-divinylbenzene. For the PS-DVB porous microspheres, the decomposition process occurred in a single stage (Fig. 4b). Given that it is a pore-forming agent, it can be inferred that the decomposition stage between 340ºC and 450ºC corresponded to the breakdown of the main chain of styrene- divinylbenzene. Two weight loss stages were also observed in the study (Fig. 4c): The dehydration stage and the pyrolysis of the main chain and sulfonic groups. During the dehydration stage, weight loss was 14.47% between 50ºC and 200ºC, while the cleavage of the main chain and sulfonic groups occurred around 400ºC, resulting in a weight loss of 15.03%. The results indicated that the self-made resin contained more high temperature-resistant components, suggesting that it retained some moisture and exhibited good thermal stability.

XRD characterization

The steamed bread peak appeared at 2θ 19.1°, which matched the polystyrene peak in the JCPDS standard card (Fig. 5). However, the crystal structure of the PS-DVB microspheres remained unchanged before and after Soxhlet extraction, indicating that only the porogen was removed during extraction and that the crystalline structure formed by the polymerization chain was not affected. The crystallization peak of the SPS-DVB-Na resin was still present, but the intensity of the steamed bread peak signal weakened. This observation suggested that the sulfonation reaction did not alter the crystal structure of the polymer microspheres.

Elemental analysis

The PS-DVB gel microspheres and porous microspheres were composed of carbon (C) and hydrogen (H) before and after Soxhlet extraction (Table 1). After extraction, the C content slightly increased, while the H content slightly decreased. Sulfur (S) was introduced during the sulfonation reaction, and the S content in the self-made resin increased to 19.89%, compared to 13.15% in the original IRP69 resin, which represented a 6.74% increase. The results suggested that the porous structure of sodium polystyrene sulfonate significantly enhanced its degree of sulfonation, leading to the introduction of more sulfonic groups during the sulfonation process, which in turn produced more exchangeable groups and increased the resin's exchange capacity.

Sodium content and potassium exchange capacity

An atomic absorption spectrometer was used to determine the sodium (Na) and potassium (K) content in the self-made samples and IRP 69 resin. Deionized water was used as a blank solution to adjust the baseline, and absorbance was measured at wavelengths of 589 nm and 769 nm, respectively. The Na content and K exchange capacity of the self-made resin were significantly higher compared to the imported IRP69 resin (Table 2). The exchange capacity of the self-made resin exceeded that of the imported resin, and it also demonstrated better drug loading performance as a pharmaceutical excipient.

Evaluation of drug resin complex

To determine the optimal drug loading process for preparing the verapamil hydrochloride drug-resin complex, the effects of temperature, drug-to-resin ratio, and drug concentration were investigated.

The drug loading rate increased as the temperature rose from 25ºC to 45ºC (Fig. 6). However, the drug loading quantity (*Q)* and drug utilization ratio (*E)* did not significantly change when the temperature reached to 37ºC. Thus, the drug loading temperature was set at 37ºC. Using drug loading and drug utilization as indicators, different drug-to-resin ratios were investigated. As shown in Fig. 7 and Fig. 8, increasing the drug-to-resin ratio led to a rise in drug loading but a decrease in drug utilization rate. This was attributed to the resin reaching a saturated state and being unable to bind additional drug. Therefore, a drug-to-resin ratio of 1:1 was determined to be optimal.

To determine the optimal drug concentration for preparing the drug-resin complex, four different concentrations of verapamil hydrochloride (1, 3, 5, and 7 mg/mL) were tested for the drug loading. The results indicated that drug concentration had little impact on the overall drug loading; however, both drug loading and drug utilization rate were highest at a concentration of 5 mg/mL (Fig. 9). Consequently, a drug concentration of 5 mg/mL was selected.

The preparation process for the verapamil hydrochloride drug-resin complex was established as follows: 50 mL of 5 mg/mL VH solution, 250 mg of self-made porous ion exchange resin, a drug loading temperature of 37ºC, and a drug loading time of 60 minutes.

In vitro drug release

In vitro release conditions

The verapamil hydrochloride resin complex requires an ion exchange within the medium to release the drug (Daihom *et al.*, 2020), making it essential for the release medium to have a certain ionic strength. To comprehensively evaluate the release behavior of the drug-resin complex and suspensions under various release conditions, this study investigated the effects of different ion types and concentrations on drug release.

Based on the single-factor analysis, the *in vitro* release conditions were established as follows: dissolution medium, 0.15 M NaCl aqueous solution; medium volume, 900mL; dissolution temperature, 37.0ºC ± 0.5ºC; and stirring speed, 50 rpm.

Table 1: Elemental content of PS-DVB gel microspheres, porous microspheres, self-made resin and IRP69 resin

Elements	Content (%)			
	PS-DVB gel microspheres	PS-DVB porous microspheres	self-made resin	IRP69 resin
C	86.06	86.68	38.30	37.70
H	7.67	7.49	4.14	4.26
N	0.00	0.00	0.00766	0.00
S	0.00	0.00	19.89	13.15

Table 2: Na content and K exchange volume measurement of different resins

Sample	Na content C (%)	K content C (g/g)
IRP69 resin	9.506	0.1107
Self-made resin	14.269	0.1681

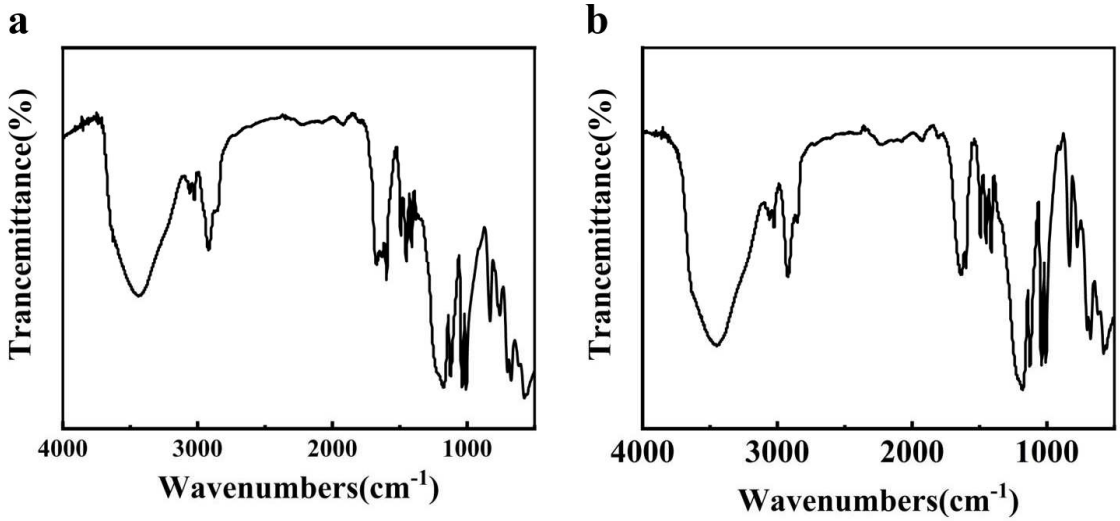

Fig. 1: Infrared spectra of self-made resin (a) and IRP69 resin (b)

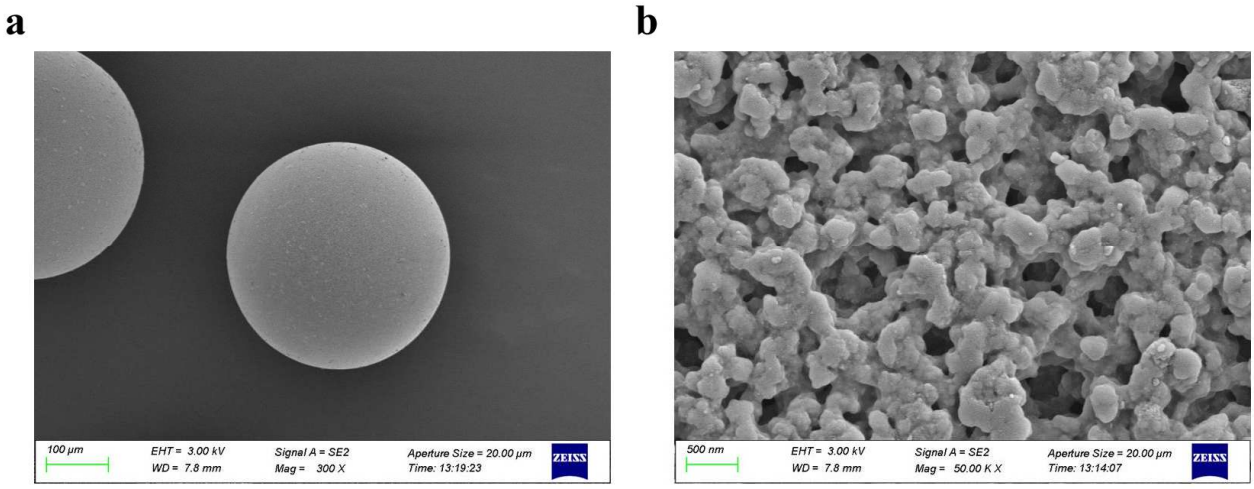

Fig. 2: SEM images of SPS-DVB-Na porous resin

Table 3: Pharmacokinetic parameters of commercial tablets and self-made VH suspension

Pharmacokinetic parameter	VH tablet	Self-made VH suspension
T_{max} (h)	2.00 ± 0.00**	5.00 ± 0.00
C_{max} (μg/mL)	2.23 ± 0.13**	1.10 ± 0.12
$t_{1/2}$ (h)	1.41 ± 0.71**	4.19 ± 0.44
$AUC_{0\text{-}24}$ (μg/mL·h)	5.14 ± 0.30	5.51 ± 1.09
MRT (h)	5.61 ± 1.44**	12.01 ± 1.31

Data are presented as mean ± SD (n = 6, **p < 0.01)

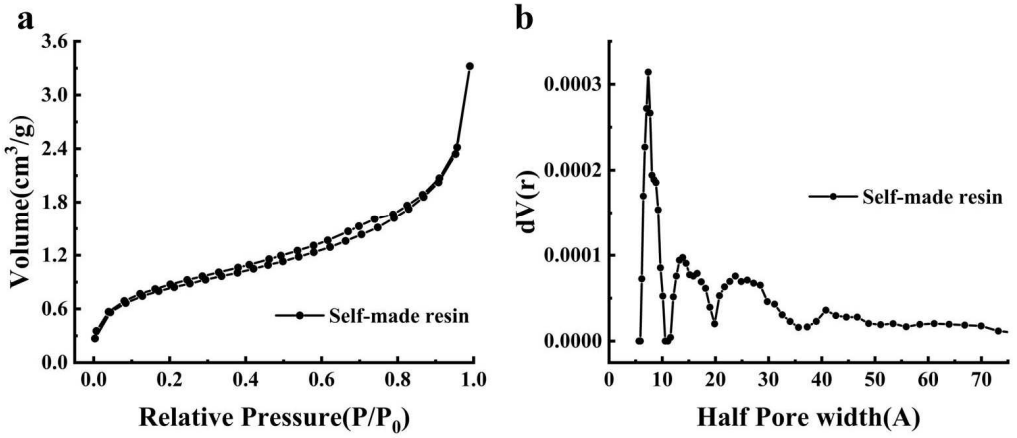

Fig. 3: The adsorption-desorption curve (a) and pore size distribution diagram (b) of porous sodium polystyrene sulfonate

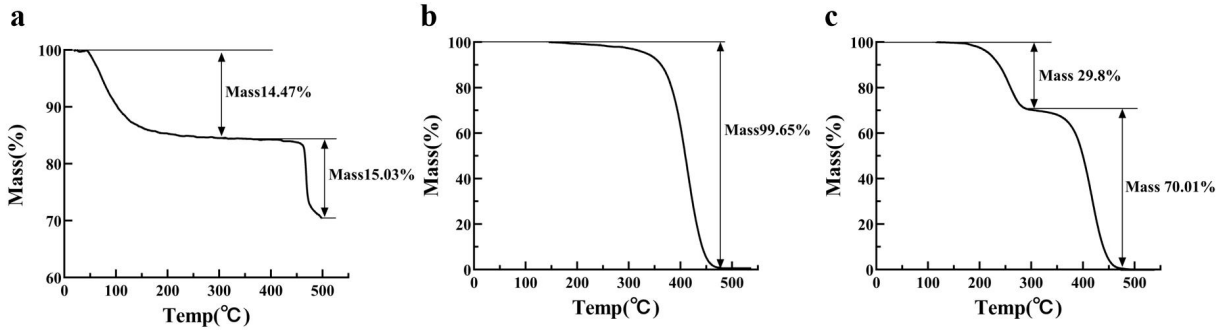

Fig. 4: Thermogravimetric curves of PS-DVB gel microspheres (a), PS-DVB porous microspheres (b) and SPS-DVB-Na porous resin (c)

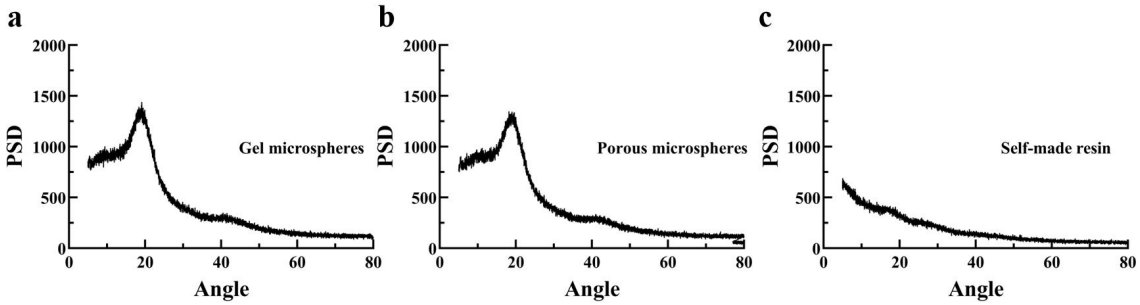

Fig. 5: X-ray diffraction patterns of PS-DVB gel microspheres (a), PS-DVB porous microspheres (b) and SPS-DVB-Na porous resin (c)

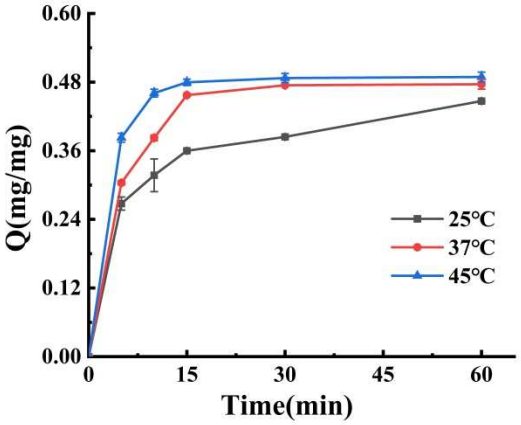

Fig. 6: The effect of temperature on drug loading (n=3)

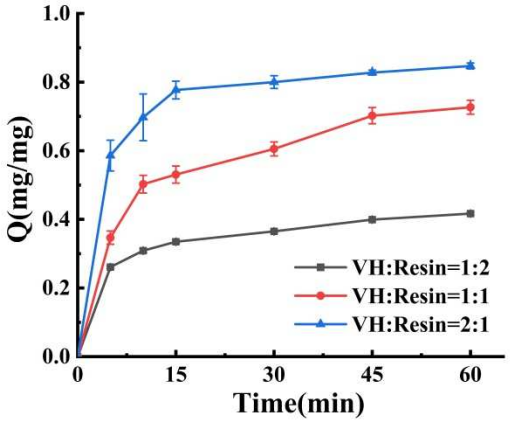

Fig. 7: The effect of drug-resin ratios on drug loading (n=3)

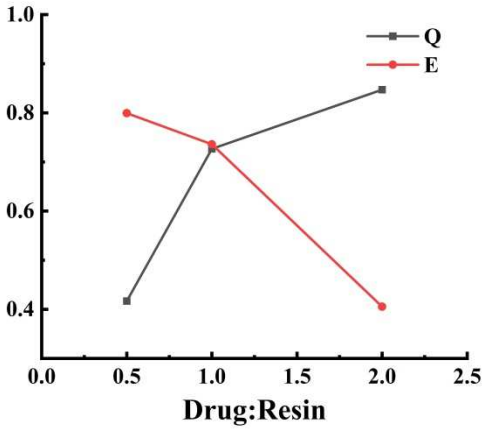

Fig. 8: Drug loading and drug utilization rate of different drug resin ratios

In vitro release of coated resin

Prior to coating, the verapamil hydrochloride resin complex demonstrated a release of less than 10% in acidic medium over a 2-hour period, but showed a rapid release in pH 6.8 phosphate buffer solution, which achieved a cumulative release of 90% (Fig. 10). The results suggested that the coating could slow the release rate of the drug-resin complex in the stomach, providing an enteric dissolution effect. The f_2 factors for the three batches of VRC-CM were all above 50, which indicated high reproducibility.

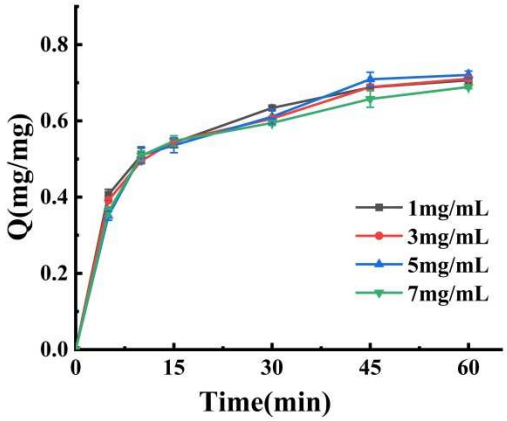

Fig. 9: The effect of drug concentration on drug loading (n=3)

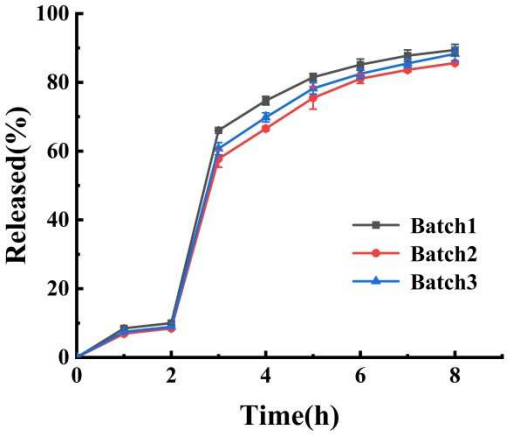

Fig. 10: *In vitro* drug release curve of three batches of self-made VRC-CM (n=3)

In vitro release of suspension

In acid medium, the release of the self-made suspension did not exceed 10% in the first 2 hours, with a final release of 85% (Fig. 11). The calculated f_2 factor for the self-made suspension was 79, indicating that its release behavior was comparable to that of VRC-CM, and achieving the expected enteric administration effect.

In vivo pharmacokinetics

The commercially available VH tablet reached peak plasma concentration (C_{max}) at 2 hours, while the self-made VH suspension reached its peak at 5 hours (Fig. 12).

The T_{max} for the self-made VH suspension was delayed from 2 hours to 5 hours. Additionally, the C_{max} decreased while, the half-life ($t_{1/2}$) increased, and the mean residence time (MRT) was also prolonged, with statistically significant differences between the two formulations ($p < 0.01$). The area under the concentration-time curve (AUC_{0-24}) slightly increased, but the difference was not statistically significant ($p \approx 0.60$) (Table 3). The relative bioavailability of the VH suspension was 107.55% of that of the tablets, with a statistically significant difference.

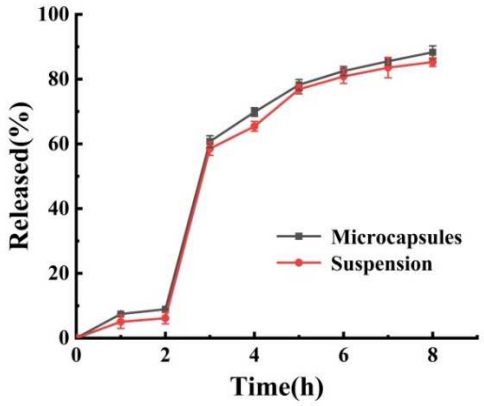

Fig. 11: *In vitro* drug release curve of self-made VRC-CM and suspension (n=3)

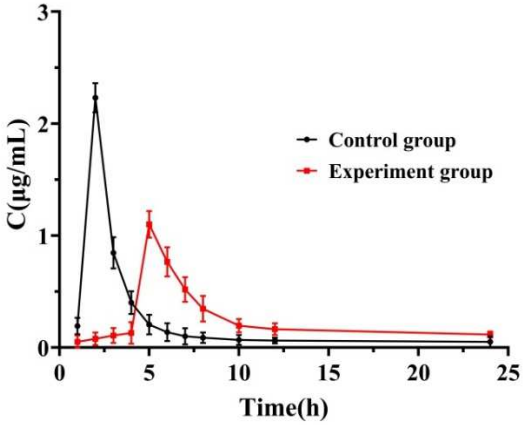

Fig. 12: Drug time curve of self-made VH suspension and commercial VH conventional tablet in SD rats (n=3)

DISCUSSION

Factors affecting ion exchange resin synthesis

Dosage of crosslinking agent

The drug loading capacity of ion exchange resins with crosslinking degrees of 10%, 20%, and 40% was investigated, and the amount of crosslinking agent optimized based on the final drug load (Fig. 13 and 14).

The results indicated that the degree of crosslinking significantly affected the morphology, particle size, and drug-loading capacity of the microspheres. The microspheres could not be formed and the product was a white emulsion solution after the polymerization when the crosslinking degree was lower than 7%. Similar findings have been reported, whereby insufficient crosslinking resulted in poor microsphere stability due to inadequate network formation hindered the formation of spherical structures (Rai *et al.*, 2016). At a crosslinking degree of 10%, although microspheres were formed, surface irregularities and cracks were observed (Fig. 13a), indicating that low crosslinking may impact structural integrity during processes such as Soxhlet extraction and sulfonation. Microspheres with a crosslinking degree of 20% exhibited both good morphology and an acceptable particle size distribution (Fig. 13b). This degree of crosslinking appeared optimal, and balancing both stability and structural integrity, which aligned with findings that moderate crosslinking degrees and improved microsphere durability without excessively reducing drug loading (Mane *et al.*, 2015). At higher crosslinking degrees (e.g., 40%), the microspheres maintained good morphology but exhibited smaller particle sizes (Fig. 13c). Drug loading was highest at a crosslinking degree of 10%, but slightly decreased at 20%, and significantly reduced at 40% (Fig. 14). The observation was due to tighter binding between microspheres, lower swelling, and reduced sulfonation. This inverse relationship between crosslinking density and drug loading capacity has been similarly noted in other studies (Uddin *et al.*, 2024). Based on these findings, a 20% crosslinking degree was chosen as optimal, with balancing morphological integrity and acceptable drug loading.

Dispersant dosage

PVA solutions of different concentrations (3, 6, and 9 mg/mL) were selected for investigation. There were uneven dispersion of substrates and wide particle size distribution of prepared microspheres (Fig. 15a, Fig. 16a) when the concentration of dispersant was too low (3 mg/mL).

Free radical polymerization was less efficient at a dispersant concentration of 9 mg/mL, which resulted in fewer products and poor sphericity (Fig. 15c, Fig. 16c). Excessive dispersant concentration inhibited effective monomer interaction and polymer network formation, leading to irregular particle shapes and reduced reaction efficiency (Yu *et al.*, 2023). However, the particle size prepared was more uniform (Fig. 15b, Fig. 16b) when the dispersant concentration was at 6 mg/mL. Therefore, 6 mg/mL PVA aqueous solution was selected as the dispersion medium of the reaction.

Dosage of initiator

The morphology of the microspheres was examined with BPO initiator concentrations of 0.5% (Fig. 17a), 1% (Fig. 17b), and 2% (Fig. 17c) relative to the monomer ST. The microspheres exhibited the best shape (Fig. 17b) when the BPO concentration was 1% of the monomer. As the BPO

Table 4: The optimized feed ratio of the first step

Phase	Chemical Name	Abbreviation	Dosage
Oil phase	Styrene	ST	13.06 mL
	Divinylbenzene	DVB	4.25 mL
	Dibenzoyl peroxide	BPO	0.1264 g
	Toluene	TOL	7.50 mL
	N-heptane	HEP	3.75 mL
	Cyclohexanol	COL	3.75 mL
Water phase	Polyvinyl alcohol	PVA	0.78 g
	Sodium chloride	NaCl	0.65 g
	Deionized water	———	130 mL

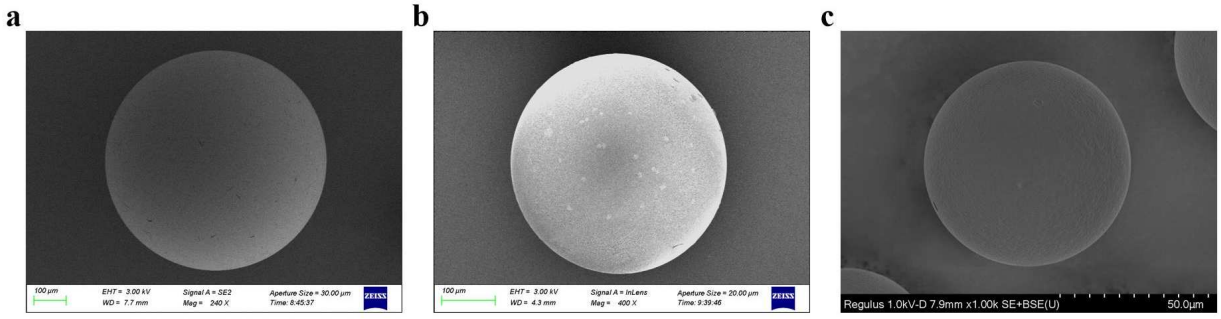

Fig. 13: The SEM images of microspheres with 10% (a), 20% (b), and 40% (c) crosslinking degree

concentration increased, the microspheres surface became uneven, and the small ball formations adhered (Fig. 17c), which could lead to the 'detonation' phenomenon of the microspheres (Cong *et al.*, 2018). Therefore, the initiator BPO concentration selected for the study was 1% of the monomer amount.

Types and dosage of pore-forming agent

Toluene-n-heptane (HEP)-cyclohexanol (Mansour *et al*., 2020), a mixture of good and poor solvents for ST-DVB, was selected as a co-porogen. The porogen-to-monomer ratio of 1:2(Fig. 18a) and 1:1(Fig. 18b) (m:m) was investigated, with toluene, n-heptane, and cyclohexanol used in a 2:1:1 (v:v) ratio.

The microspheres prepared using the optimal synthesis conditions, and determined through the single-factor investigation, exhibited good shape. However, due to the small molecular weight of the liquid pore-forming agent, the pore size formed was small (Liu *et al.*, 2022a). Scanning electron microscopy at low magnification could not determine whether the microspheres contained a pore structure, so higher magnification was used for characterization.

Under higher magnification scanning, the surface structure of the microspheres was not clearly defined when the amount of pore-forming agent was low (Fig. 19a). However, when the amount of pore-forming agent was equal to the amount of monomer, the surface structure became more distinct (Fig. 19b). The pore-forming agent used was a mixture of good and poor solvents, and it was difficult to form a pore structure when the amount was low. A loose structure of microspheres can increase the specific surface area, enhance the average pore size, and improve pore volume. However, an excessive amount of pore-forming agent can lead to an unstable microsphere structure during sulfonation after Soxhlet extraction. Similar findings have been documented in previous studies, indicating that maintaining structural stability requires an optimal concentration of pore-forming agents (Zhuang *et al*., 2024).

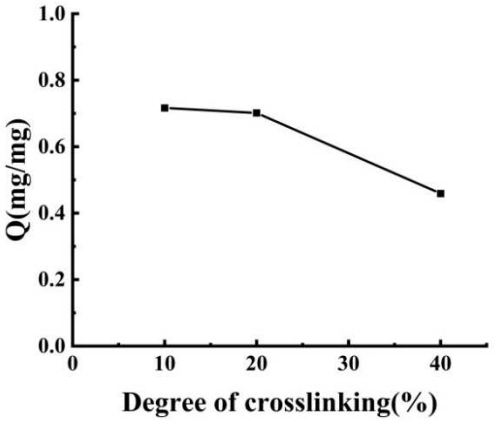

Fig. 14: The effect of cross-linking degree on the drug loading of microspheres

Type and dosage of sulfonating agent

In this study, concentrated sulfuric acid was selected as the sulfonation reagent (Xu *et al*., 2022), and the degree of sulfonation of the final product was determined by

Table 5: The optimized feed ratio of the second step

Chemical Name	Dosage
Porous PS-DVB microspheres	2.0045 g
Chloroform	10 mL
Concentrated sulfuric acid	4 mL
Deionized water	100 mL
Acetone	5mL*2

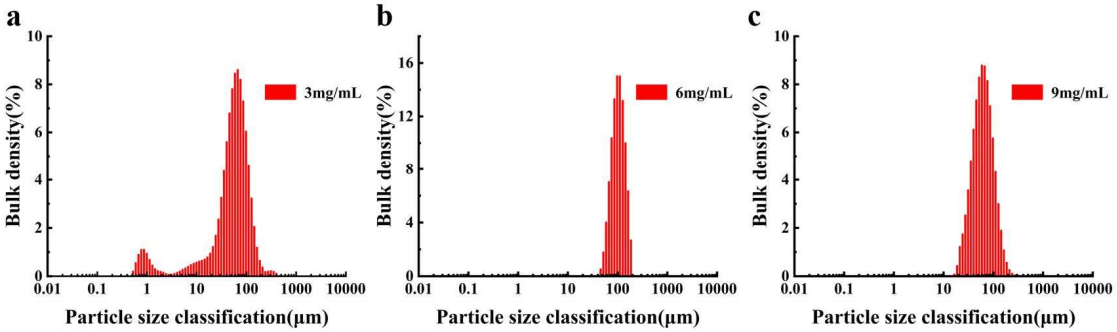

Fig. 15: The particle size distribution of microspheres with dispersant concentrations of 3 mg/mL (a), 6 mg/mL (b), and 9 mg/mL (c)

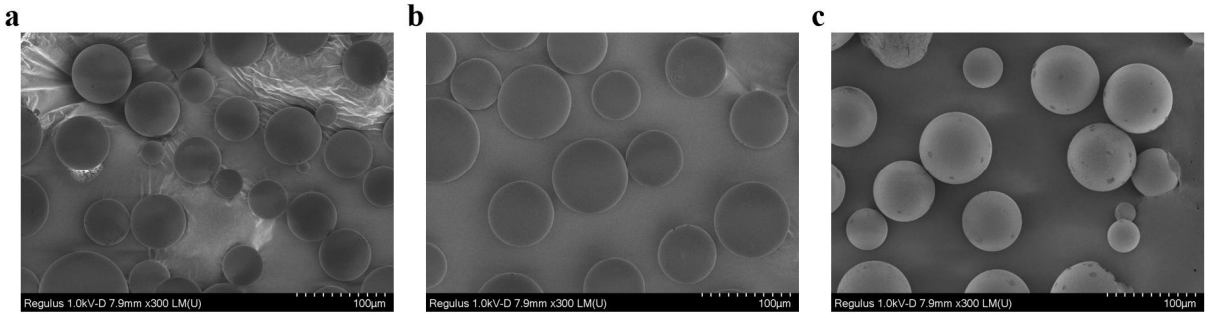

Fig. 16: SEM images of microspheres with dispersant concentrations of 3 mg/mL (a), 6 mg/mL (b), and 9 mg/mL (c)

measuring the amount of NaOH consumed in an alkaline titration. As the concentration of sulfuric acid increased, the degree of sulfonation of the microspheres also increased, although the change was not significant (Fig. 20). Considering the safety and environmental concerns associated with the sulfonation reaction, the amount of sulfonating agent (mL) was ultimately determined to be three times the weight of microspheres (g).

Optimized feeding scheme

The reaction conditions of polymerization were determined by investigating the single factor experiments. The final feed quantity is shown in Tables 4 and 5.

In vivo pharmacokinetics

The sustained-release suspension, after gastric emptying into the intestines and exposure to the change in environmental pH, triggered a burst release of the enteric coating material, which achieved a pulsed release effect (Pawar and Varsha, 2018). This burst release occurred after the peak concentration due to the slow-release nature of the ion-exchange resin. The results aligned with the expected pulse slow-release effect (Dasankoppa *et al*., 2016), which demonstrated that the plasma drug concentration of the self-made suspension was more stable, with improved safety and prolonged effective action time. However, several limitations of the present study should be acknowledged. Thus, the *in vivo* experiment involved a relatively small sample size, which may limit the generalizability of the findings. Furthermore, long-term stability testing was not conducted, which was critical for assessing the sustained-release formulation's performance over time.

CONCLUSION

In this study, porous cation exchange resin sodium polystyrene sulfonate was prepared through suspension polymerization and sulfonation, which resulted in a resin with high specific surface area and exchange capacity.

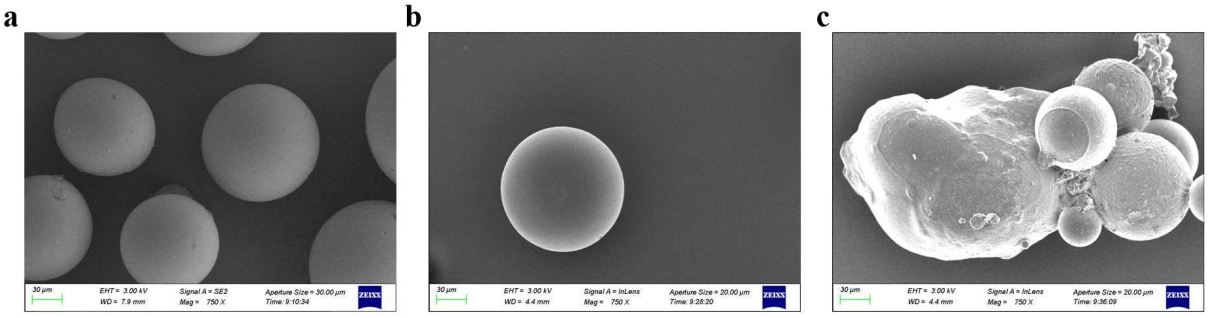

Fig. 17: SEM images of microspheres prepared with initiator concentrations of 0.5% (a), 1.0% (b), and 2.0% (c)

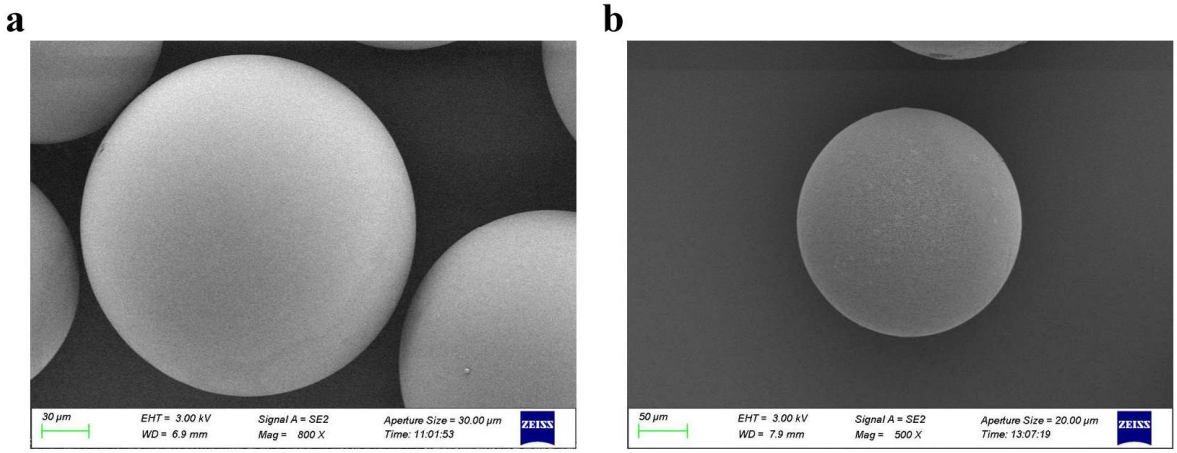

Fig. 18: SEM images of microspheres with different porogen concentrations and porogen-to-monomer ratios of 1:2 (a) and 1:1 (b)

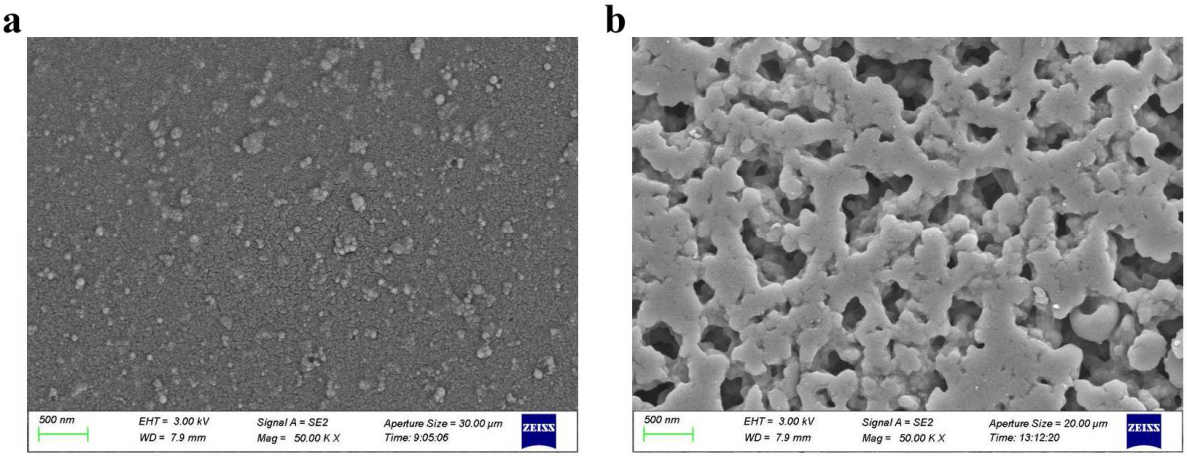

Fig. 19: SEM images of microspheres prepared with different porogen concentrations (reduced size), with porogen-to-monomer ratios of 1:2 (a) and 1:1 (b)

The resin was used as a carrier to prepare VRC, which was then impregnated and coated to form a suspension. Commercial VH tablets served as the reference. The results showed that the relative bioavailability of both preparations (commercial tablets and self-made suspension) was bioequivalent (Liu *et al*., 2022b). Furthermore, compared to the conventional drug, the self-made suspension exhibited delayed peak time, increased half-life, reduced maximum plasma concentration, improved safety, prolonged effective time, and a distinct pulse-sustained release effect.

The porous cation exchange resin developed in this study demonstrated excellent properties and significant

application potential. The pulse-sustained release suspension produced using the superior resin as a key excipient offered an innovative approach for developing verapamil hydrochloride delivery systems, which provided new perspectives for formulation strategies. Future research should focus on optimizing the controlled-release mechanisms to enhance drug release profiles and extend therapeutic effects. Additionally, the scalability and long-term stability of resin-based delivery systems require further exploration, as these factors are essential for successful clinical translation. These areas of research will be crucial in advancing controlled-release drug delivery and improving the therapeutic efficacy of sustained-release formulations.

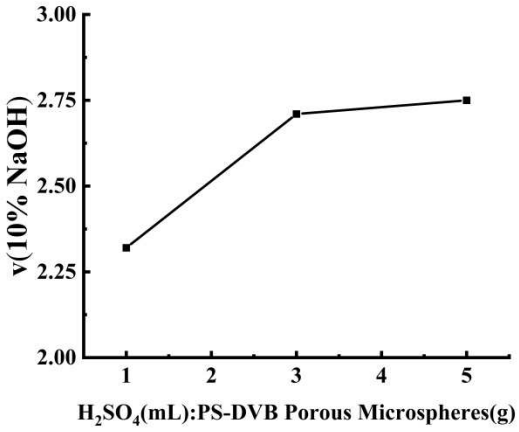

Fig. 20: Investigation of different dosages of sulfonating agent

Acknowledgements
This work was supported by 2022 New Drugs and Platform Enhancement Project of the Yangtze Delta Drug Advanced Research Institute, 2023 Nantong Jianghai Talent Plan (No 2023A053), Nantong Social Livelihood Science and Technology Plan for 2023, 2021 Zhenjiang sixth "169 project" scientific research project, 2023 Qinglan Project of Jiangsu Province of China, Jiangsu Province Engineering Research Center of Surface Interface Functional Composites, Jiangsu Higher Vocational College Engineering Research Center of Green Energy and Low Carbon Materials,

Authors' contributions
Wei Mi: Writing-review & editing, Writing-original draft, Methodology, Formal analysis, Data curation, Conceptualization. Tao Xiao: Writing-review & editing, Writing-original draft, Methodology, Formal analysis, Data curation, Conceptualization. Yang Xu: Writing-original draft, Methodology, Formal analysis, Data curation, Conceptualization. Jiapeng Wang: Methodology, Formal analysis, Data curation. Yingshu Feng: Writing-review & editing, Formal analysis, Conceptualization. Caleb Kesse Firempong: Writing-review & editing, Formal analysis. Yan Jiang: Writing-review & editing, Formal analysis. Haibing He: Writing-review & editing, Methodology, Formal analysis, Conceptualization. Hongfei Liu: Writing-review & editing, Methodology, Conceptualization, Funding acquisition.

Funding
There was no funding.

Data availability statement
Data available on request from the authors.

Ethical approval
This study was approved by the Ethics Committee of Jiangsu University, and the ethics approval number was 202213643.

Conflict of interest
The authors declare no conflict of interest.

REFERENCES

Allaboun H, Alkhamis KA and Al-Nimry SS (2023). Preparation of sustained release formulation of verapamil hydrochloride using ion exchange resins. *AAPS PharmSciTech*., **24**(5): 114.

Aronow WS (2020). Managing the elderly patient with hypertension: Current strategies, challenges, and considerations. *Expert Rev Cardiovasc Ther.*, **18**(2): 117-125.

Cong H, Yu B, Gao L, Yang B, Gao F, Zhang H and Liu Y (2018). Preparation of morphology-controllable PGMA-DVB microspheres by introducing Span 80 into seed emulsion polymerization. *RSC Adv.*, **8**(5): 2593-2598.

Daihom BA, Bendas ER, Mohamed MI and Badawi AA (2020). Domperidone resinate complex as new formulation for gastroretentive drug delivery. *J. Drug Deliv. Sci. Technol.*, **58**(1): 101868.

Dasankoppa FS, Komal S, Sholapur HN, Nanjundaswamy NG and Sajjanar VM (2016). Design, optimization and evaluation of chewable tablets of clarithromycin using ion exchange resins. *Indian J. Pharm. Sci.*, **78**(6): 818-826.

Deng Y, Wang T, Li J, Sun W, He H, Gou J, Wang Y, Yin T, Zhang Y and Tang X (2020). Studies on the *in vitro* ion exchange kinetics and thermodynamics and *in vivo* pharmacokinetics of the carbinoxamine-resin complex. *Int. J. Pharm.*, **588**(1): 119779.

Faisal MM, Gomaa E, Ibrahim AE, El Deeb S, Al-Harrasi A and Ibrahim TM (2024). Verapamil-loaded cubosomes for enhancing intranasal drug delivery: Development, characterization, ex vivo permeation, and brain biodistribution studies. *AAPS PharmSciTech.*, **25**(5): 95.

Gaur P K, Mishra S, Bhardwaj S, Puri D and Kumar S S (2014). Ion exchange resins in gastroretentive drug

delivery: characteristics, selection, formulation and applications. *J. Pharm. Sci. Pharmacol.*, **1**(4): 304-312.

Han M, Du Y, Wu X, Zhang X, Yang Q, Firempong CK, Liu H and Li D (2023). Development, optimization, and *in vitro/in vivo* evaluation of ranitidine hydrochloride-resinate sustained-release suspension. *Trop. J. Pharm. Res.*, **22**(3): 457-467.

Lei YL, Luo YJ, Chen F and Mei LH (2014). Sulfonation process and desalination effect of polystyrene/PVDF semi-interpenetrating polymer network cation exchange membrane. *Polymers.*, **6**(7): 1914-1928.

Leonova MV (2020). Opportunities of chronotherapy use in treatment of arterial hypertension and comorbid disorders. *Cons Med.*, **22**(1): 31-37.

Li C, Han X, Hong X, Li X, Zhang H, Wang Z and Zheng A (2021). Study on the complexation and release mechanism of methylphenidate hydrochloride ion exchange resin complex. *Polymers.*, **13**(24): 4394.

Liu H, Xie X, Chen C, Firempong CK, Feng Y, Zhao L and Yin X (2021). Preparation and in vitro/in vivo evaluation of a clonidine hydrochloride drug–resin suspension as a sustained-release formulation. *Drug Dev. Ind. Pharm.*, **47**(3): 394-402.

Liu H, Lai X, Chen C, Feng Y, Yu Y, Yin X and He H (2022). Preparation, characterization of clonidine hydrochloride resinates and investigation of the kinetics and thermodynamics of the ion exchange process. *Pak. J. Pharm. Sci.*, **35**(3): 721-729.

Liu H, Zou Y, Zhu J, He H, Feng Y, Firempong CK, Yu Y and Sun C (2022). Preparation and evaluation of rhINF-α-2b sodium hyaluronate cross-linked porous microspheres: Characterization, sustained-release properties, and antitumor activity. *AAPS PharmSciTech.*, **23**(1): 31.

Mane S, Ponrathnam S and Chavan N (2015). Effect of chemical cross-linking on properties of polymer microbeads: A review. *Can. Chem. Trans.*, **3**(4): 473-485.

Mansour FR, Waheed S, Paull B and Maya F (2020). Porogens and porogen selection in the preparation of porous polymer monoliths. *J. Sep. Sci.*, **43**(1): 56-69.

Moeed A, Khalid A, Bashir S, Bashir H, Al Kahraman YM, Ismail T and Amirzada MI (2021). Verapamil hydrochloride nanoparticles formulated with chitosan and sodium alginate by an ionic gelation method. *Trop. J. Pharm. Res.*, **20**(6): 1105-1111.

Mohammed SS and Babu N (2015). Formulation development and evaluation bilayer floating sustained and immediate release tablet of verapamil hydrochloride by direct compression method. *Res. J. Pharm. Technol.*, **8**(5): 539-548.

Panraksa P, Boonsermsukcharoen K, Hwang KM, Park ES and Jantrawut P (2019). Taste masking of nizatidine using ion-exchange resins. *Processes*., **7**(11): 779.

Pawar P and Varsha G (2018). Formulation and evaluation of mesalamine loaded pH dependent colon specific pulsatile drug delivery system. *Curr. Res. Pharm. Sci.*, **8**(3): 244-253.

Qin F, Zeng L, Zhu Y, Cao J, Wang X and Liu W (2016). Preparation and evaluation of a timolol maleate drug-resin ophthalmic suspension as a sustained-release formulation *in vitro* and *in vivo*. *Drug Dev. Ind. Pharm.*, **42**(4): 535-545.

Qu Y, Lai WL, Xin YR, Zhu FQ, Zhu Y, Wang L, Ding YP, Xu Y and Liu HF (2019). Development, optimization and evaluation in vitro/in vivo of oral liquid system for synchronized sustained release of levodopa/benserazide. *AAPS PharmSciTech.*, **20**(8): 312.

Rai G, Yadav AK, Jain NK and Agrawal GP (2016). Eudragit-coated dextran microspheres of 5-fluorouracil for site-specific delivery to colon. *Drug Deliv.*, **23**(1): 328-337.

Rajesh AM and Popat KM (2017). Taste masking of ofloxacin and formation of interpenetrating polymer network beads for sustained release. *J. Pharm. Anal.*, **7**(4): 244-251.

Rajesh AM, Bhatt SA, Brahmbhatt H, Anand PS and Popat KM (2015). Taste masking of ciprofloxacin by ion-exchange resin and sustain release at gastric-intestinal through interpenetrating polymer network. *Asian J. Pharm. Sci.*, **10**(4): 331-340.

Ramu B, Kumar SU, Srikanth G and Rajkamal B (2016). Formulation and evaluation of sustained release verapamil hydrochloride using natural polymers. *Int. J. Appl. Pharm. Sci. Res.*, **1**(02): 76-87.

Sivaneswari S, Veena D, Sumana PS, Subhashree P, Ramya L, Rajalakshmi R, Chandana PJ and Karthikeyan E (2015). Ion exchange resins as drug delivery carriers. *J. Chem. Pharm. Res*, **7**(4): 1436-1445.

Shaik I, Gopinath H, Bhowmik D and Khirwadkar P (2015). Formulation and evaluation of osmotic controlled release verapamil tablets. *Indian J. Res. Pharm. Biotechnol.*, **3**(1): 28.

Uddin MS, Khand S and Dong C (2024). Effect of crosslinking agents on chitosan hydrogel carriers for drug loading and release for targeted drug delivery. *Gels.*, **10**(7): 421.

Xie F, Ji S and Cheng Z (2015). *In vitro* dissolution similarity factor (f2) and *in vivo* bioequivalence criteria, how and when do they match? Using a BCS class II drug as a simulation example. *Eur. J. Pharm. Sci*., **66**(1): 163-172.

Xu H, Liu B and Zhang M (2022). Preparation and application of monodisperse, highly cross-linked, and porous polystyrene microspheres for dye removal. *Colloids Surf. A Physicochem. Eng. Asp.*, **650**(1): 129596.

Yin R, Yin L, Li L, Silva-Nash J, Tan J, Pan Z, Zeng J and Yan LL (2022). Hypertension in China: Burdens, guidelines and policy responses: A state-of-the-art review. *J. Hum. Hypertens.*, **36**(2): 126-134.

Yu H, Liu J, Zhao L, Liu Y, Gu L, Feng L and Qu J

(2023). Synthesis of acrylic resin and methacrylic resin microspheres by suspension polymerization. *Front. Chem.*, **11**(1): 1193553.

Yuan J, Li C, Wang S, Zhang H, Wang Z, Zheng A and Gao X (2023). Methods and characteristics of drug extraction from ion-exchange-resin-mediated preparations: influences, thermodynamics, and kinetics. *Polymers.*, **15**(5): 1191.

Zhang TY, Du RF, Wang YJ, Hu JL, Wu F and Feng Y (2022). Research progress of preparation technology of ion-exchange resin complexes. *AAPS PharmSciTech.*, **23**(4): 105.

Zhou M, Shen L, Lin X, Hong Y and Feng Y (2017). Design and pharmaceutical applications of porous particles. *RSC Adv.*, **7**(63): 39490-39501.

Zhuang S, Jin X, Cen L and Shao Y (2024). Encapsulation of hydroxycamptothecin within porous and hollow poly (L-lactide-co-ε-caprolactone) microspheres as a floating delivery system for intravesical instillation. *Biomater Sci.*, **12**(14): 3659-3671.